PUBLICATION II

Microstructural characterisation of thermally sprayed quasicrystalline Al-Co-Fe-Cr coatings

In: Journal of Alloys and Compounds 2003.
Vol. 354, No. 1–2, pp. 269–280.

ELSEVIER

Journal of Alloys and Compounds 354 (2003) 269–280

Journal of ALLOYS AND COMPOUNDS

www.elsevier.com/locate/jallcom

Microstructural characterisation of thermally sprayed quasicrystalline Al–Co–Fe–Cr coatings

E. Huttunen-Saarivirta[a,*], E. Turunen[b], M. Kallio[c]

[a]*Tampere University of Technology, Institute of Materials Science, P.O. Box 589, Fin-33101, Tampere, Finland*
[b]*VTT Technical Research Centre of Finland, Surface Engineering and Laser Processing, P.O. Box 1703, Fin-02044 VTT, Tampere, Finland*
[c]*VTT Technical Research Centre of Finland, Materials and Chemicals, Hermiankatu 8 G, P.O. Box 16071, Fin-33101, Tampere, Finland*

Received 20 November 2002; accepted 4 December 2002

Abstract

A microstructural characterisation was carried out for Al–Co–Fe–Cr feed powder and the coatings sprayed with a high velocity oxy-fuel method using different operation conditions. The aims of the study were to explore the structural development of thick Al–Co–Fe–Cr coatings and the influence of the spraying parameters on the microstructure of produced Al–Co–Fe–Cr coatings. X-ray diffractometry, scanning electron microscopy and analytical transmission electron microscopy were the techniques used in the phase identification and in the microstructural exploration of the study. The results show that Al–Co–Fe–Cr feed powder and the coatings sprayed with low and high operation temperature are composed of a dodecagonal quasicrystalline phase. The composition of this new dodecagonal phase approximately corresponds to that of the feed powder, being $Al_{70.6}Co_{12.5}Fe_{9.4}Cr_{7.5}$. The dodecagonal phase does not decompose during the spraying process. Instead, it orientates to form a lamellar coating structure. When a lower spraying temperature is used, the incomplete melting of powder particles introduces a partly orientated coating structure. Due to this incomplete melting of powder particles, porosity is also involved in these coatings. Higher spraying temperature, in turn, promotes oxidation, leading to the incorporation of an oxygen-containing film on the splat boundaries. While the feed powder and the coating deposited with a lower spraying temperature are one-phase quasicrystalline structures, the coating sprayed with a higher operation temperature is comprised of a dodecagonal phase and an oxygen-containing phase. This oxygen-containing phase is not pure aluminium oxide but contains all the elements present in the alloy.

Keywords: Transition metal alloys; Quasicrystals; Coating materials; TEM; SEM

1. Introduction

Quasicrystals are materials where a repeating periodicity in an atom arrangement exists together with a rotational symmetry forbidden for crystalline materials; fivefold, eightfold, tenfold and even twelvefold symmetries have been encountered in quasicrystals [1]. The first observation of a fivefold symmetry in a rapidly-solidified Al–Mn alloy in 1984 [2] triggered an intense theoretical study of quasicrystals. The examination of a new and exceptional structure of quasicrystals, the survey of their physical and mechanical properties and the development of theories explaining the observed qualities have been the central academic research topics during the last two decades. However, the focus of the research is currently shifting closer to the reality; much interest is nowadays concentrated on finding practical production techniques and applications for these materials.

The first method used to prepare quasicrystalline phases was melting followed by a rapid quenching using the melt spinning technique [2]. Nowadays the fabrication of quasicrystalline materials is possible by a number of different manufacturing methods making use of the variety of the solidification rates of melt [3,4], powder metallurgical processes [5–7] and thin film techniques [8–12]. Besides quasicrystals in bulk, powder or thin film form

*Corresponding author. Tel.: +358-3-365-2912; fax: +358-3-365-2330.
E-mail address: elina.huttunen-saarivirta@tut.fi (E. Huttunen-Saarivirta).

0925-8388/02/$ – see front matter
doi:10.1016/S0925-8388(02)01361-0

introduced by these synthesis methods, quasicrystalline coatings with greater thickness are pursued in order to get the full advantage of the attractive combination of surface characteristics associated with quasicrystalline materials: a low surface energy [13–15], a low coefficient of friction [14,16], a good corrosion resistance [13], a high hardness [1,17,18] and a good abrasive wear resistance [19]. Thermal spraying has been shown [20–25] to be a versatile method for producing thick quasicrystalline coatings with these qualities.

So far, the majority of studies on the thermally sprayed quasicrystalline coatings have concentrated on the different modifications of the ternary base alloys Al–Cu–Fe and Al–Ni–Co [21–27]. In this study, the quasicrystalline coatings of a quaternary alloy Al–Co–Fe–Cr are produced by a high velocity oxy-fuel (HVOF) spraying technique. Although the formation of a quasicrystalline structure in thin films of this alloy has been reported after heat treatments [28,29], no studies deal with the structural development of thick Al–Co–Fe–Cr coatings. Another unknown area is the influence of spraying parameters on the microstructure of Al–Co–Fe–Cr coatings deposited by thermal spraying.

The aim of this study is to extract this lack of scientific data on the formation of microstructure in Al–Co–Fe–Cr thermally sprayed coatings. In the current study, thermally sprayed quasicrystalline Al–Co–Fe–Cr coatings are produced from an Al–Co–Fe–Cr feed powder by the HVOF spraying technique with two different operation conditions. The phases in the feed powder and in the formed thick coatings are identified and the sensitivity of coating microstructure to the spraying conditions such as temperature is examined. X-ray diffractometry (XRD), scanning electron microscopy (SEM) and analytical transmission electron microscopy (ATEM) are used for the microstructural characterisation of Al–Co–Fe–Cr feed powder and HVOF sprayed coatings.

2. Experimental procedure

2.1. Preparation of coatings

Al–Co–Fe–Cr coatings were applied on low carbon steel substrates by a high velocity oxy-fuel (HVOF) spraying technique. HVOF spraying technique is a thermal spraying method, where the spray powder is fed to a gas flow of high pressure, and which yields coatings of low porosity and, thus, good surface properties [30]. In the present study, the spray powder was a commercial powder Christome BT1 manufactured by Saint-Gobain Advanced Ceramics SNMI, France. The composition of the powder, given by the manufacturer, was 52.8 wt.% Al, 20.4 wt.% Co, 15.3 wt.% Fe and 11.2 wt.% Cr, which corresponds to the composition 70.1 at.% Al, 12.4 at.% Co, 9.8 at.% Fe and 7.7 at.% Cr. The particle size of the powder ranged from 20 to 53 μm.

The coatings were sprayed using a HV-2000 spray gun by Praxair Surface Technologies (USA). The gun was operated by a Model 3440 console utilising a model 1262 volumetric powder feeder by Plasmatron Pvt. Ltd. (USA). A two-axis traverse unit with a rotating spindle of a 200 mm inner diameter was used to manipulate the gun and substrates during the coating deposition. The spray distance was 300 mm in the spraying experiments of the study. In the HVOF process, nitrogen was used as a carrier gas, along with hydrogen as a fuel gas. The coatings were sprayed under two different operation conditions, varying the flow of hydrogen and oxygen and their ratio. The gas flow ratio generally determines the temperature of the flame [30], the higher oxygen content promoting the higher flame temperature. This also applied to the HVOF spraying process of the study. The thickness of the HVOF sprayed coatings also varied as a result of different operating conditions. The spraying conditions used in the study and the resulting coating thicknesses are shown in Table 1.

Temperature of the sprayed particles was studied through the spraying diagnostics. SprayWatch 2i imaging system from Oseir Ltd. (Finland), designed for the quality control of industrial thermal spray processes, was used for the on-line measurements of in-flight particles' temperature in the spray. It has to be noticed that these temperature measurements conducted during the spraying experiments only introduced the surface temperature of powder particles. Due to the low thermal conductivity of the powder particles, however, the true temperature of the inner part of particles cannot be evaluated. For the same reason, the temperature difference measured between the surfaces of particles does not correspond to the true temperature difference between the inner parts of the particles. The surface temperature of powder particles, thus, only gives a rough approximation about the scale of temperature the powder particles reach during the spraying process. The observations on the microstructural characteristics of studied Al–Co–Fe–Cr coatings deposited under different operating conditions further support these suggestions about the greater temperature difference as measured between the powder particles sprayed with different gas flow conditions.

Table 1
HVOF spraying conditions and the resulting coating thicknesses

Coating	O_2 l/min	H_2 l/min	H_2/O_2 ratio	Surface temperature of powder particles, °C	Thickness, μm
A	235	665	2.83	1950	470
B	280	620	2.21	1980	250

2.2. Microstructural characterisation of coatings

The microstructural characterisation of Al–Co–Fe–Cr coatings was performed by X-ray diffraction (XRD) measurements, scanning electron microscopy (SEM) and analytical transmission electron microscopy (ATEM). XRD measurements were carried out using a model Diffrac 500 diffractometer by Siemens (Germany) and copper Kα radiation. The XRD analyses were performed with powdery samples. Thus, the studied coatings were stripped off their substrates and crushed into powdery form in a mortar. In addition to the powdery coating samples, the feed powder was characterised by XRD in order to reveal the possible phase transitions introduced by the coating process. The microstructure of the feed powder and the sprayed coatings was also studied with a scanning electron microscope model XL30 by Siemens (The Netherlands), equipped with an energy dispersive spectrometer (EDS) model DX-4 by EDAX International (USA). The cross-sectional samples were used in the SEM studies. The feed powder and the sprayed coatings were further examined by an analytical transmission electron microscope JEM 2010 by JEOL (Japan) equipped with a Noran Vantage energy dispersive spectrometer by ThermoNoran (The Netherlands). The ATEM was operated at an accelerating voltage of 200 kV. ATEM examination was conducted for powdery samples; the coating samples were prepared similarly as for the XRD analyses.

3. Results and discussion

3.1. XRD analysis

In the XRD analysis, the feed powder and the powdery samples of coatings A and B were characterised in order to identify the compounds and phases they are composed of. In addition to the phase qualification, the aim of the XRD measurements was to reveal the possible phase transitions introduced by the coating process.

Fig. 1 shows the XRD patterns for the Al–Co–Fe–Cr feed powder and the HVOF sprayed coatings A and B. For all these samples, the peak with the highest intensity appears at about 43.5° in 2θ scale. Comparing the trace from the feed powder (Fig. 1(a)) to the trace obtained from the HVOF sprayed coatings (Figs. 1(b) and (c)) reveals microstructural evolution to take place during spraying; the intensity of the highest-intensity-peak has increased during the spraying operation. The location of the peaks does not change prominently, thus, no reaction is proposed to take place. However, the number of peaks and the intensities related to them somewhat change during the spraying of the feed powder. For the feed powder, the number of peaks in the XRD spectrum totals almost ten. In contrast, only five distinguishable peaks can be noticed in the XRD patterns of the HVOF sprayed coatings; mainly the small peaks are erased from the XRD spectra due to spraying. These findings are proposed to be linked to the texture evolution. The microstructural development during the

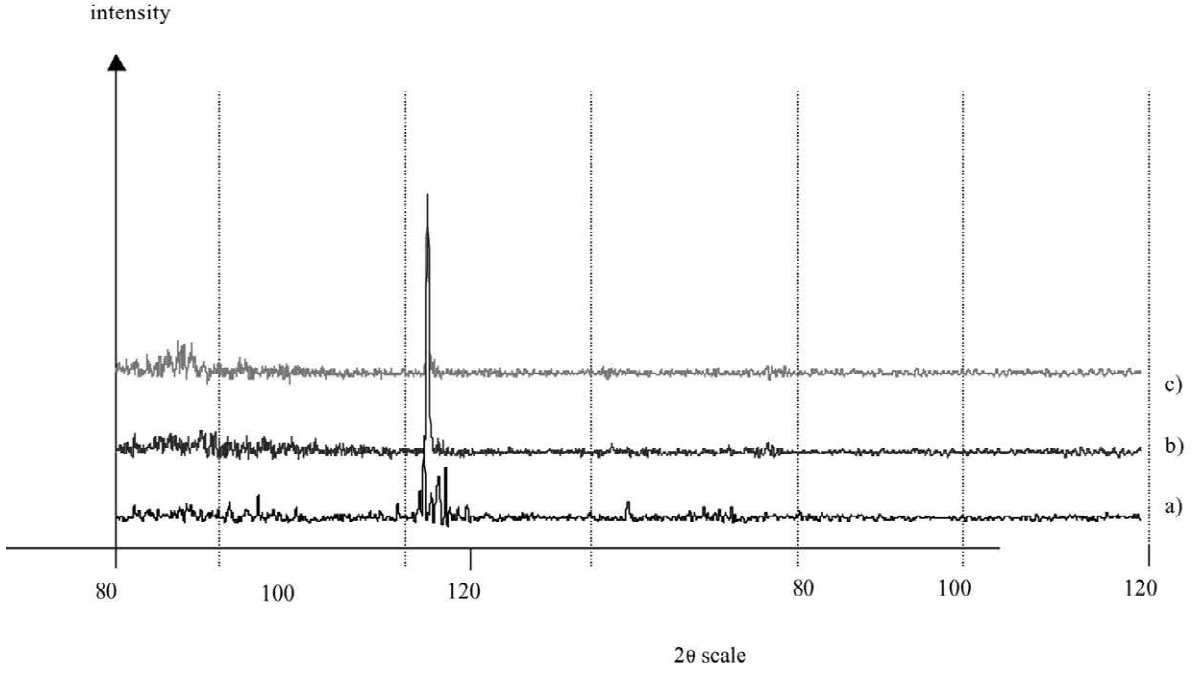

Fig. 1. XRD patterns for (a) Al–Co–Fe–Cr spray powder, (b) the Al–Co–Fe–Cr coating A sprayed with the lower spraying temperature, (c) the Al–Co–Fe–Cr coating B sprayed with the higher spraying temperature.

spraying is, accordingly, thought to be brought about by the orientation of grains during the spraying to yield texture into coatings. Besides, the small number of peaks observed in the XRD spectra of the feed powder and specially the HVOF sprayed coatings allows us to assume that only one or a maximum of two phases can create them.

The feed powder BT1 has earlier been analysed with XRD by Reyes-Gasga et al. [28,29]. They suggest the powder to be composed of Co_2O_3, $A1_2O_3$, Al_2Co_2, $A1_{86}Cr_{14}$ and $A1_{80}Cr_{20}$. From these compounds and alloys, $A1_{86}Cr_{14}$ and $A1_{80}Cr_{20}$ are quasicrystalline with fivefold rotational symmetry and, accordingly, icosahedrally structured. Applying this analysis of Reyes-Gasga et al. to the XRD patterns of the feed powder and the HVOF sprayed coatings A and B of this study indicates that they should mainly be composed of $A1_{86}Cr_{14}$ because the major peak in their XRD pattern corresponds to this quasicrystalline alloy. However, the smaller peaks of the coatings can not be connected to $A1_{86}Cr_{14}$ or any other of the named compounds or alloys. This fact as well as the perception that Fe is not included in any of the components suggested by Reyes-Gasga et al. [28,29] emerged; the feed powder and the coatings of the study are not composed of any of the compounds or alloys proposed by Reyes-Gasga et al. [28,29].

In thin films synthesised from the feed powder BT1, Reyes-Gasga et al. [28,29] observed a quasicrystalline decagonal phase $A1_{58}Cr_{20}O_{17}Fe_5$. However, knowing the existence and composition of this decagonal phase and the availability of numerous crystalline phases and intermetallic compounds for the system Al–Co–Fe–Cr, no matching of their JCDPS cards with the XRD spectra of feed powder BT1 and the HVOF sprayed coating A and B was obtained. Finally, a question about the contents of the JCDPS card files arose; what phases, compounds and alloys are really included in them? It appeared that from quasicrystalline materials, basically icosahedral phases are considered by the JCDPS card files. Octagonal, decagonal or dodecagonal phases, at least those related to Al–Co–Fe–Cr system, were ignored. It was, thus, considered whether the feed powder and the HVOF sprayed coatings of the present study could be octagonal, decagonal or dodecagonal; it was, at least, realised that they did not exhibit any known crystalline structure.

3.2. SEM studies

The aim of SEM studies was to answer questions about the coating microstructure and the phases present in the feed powder as well as in the HVOF sprayed coatings. The microstructure of the Al–Co–Fe–Cr feed powder and coatings deposited with different spraying temperatures was determined from the cross-sectional samples.

The feed powder consists of spherical particles, as shown in Fig. 2(a). SEM studies both in SE and BSE mode indicated powder particles to be composed of one phase only. This phase consisted of 71.0 at.% Al, 12.4 at.% Co, 9.2 at.% Fe and 7.5 at.% Cr. The composition of this phase, consequently, corresponds well with the powder composition given by the manufacturer.

Figs. 2(b) and (c) addresses the influence of spraying temperatures on the microstructure of Al–Co–Fe–Cr coatings. The microstructure of Al–Co–Fe–Cr coating A sprayed with lower spraying temperature is shown in Fig. 2(b). No perfectly lamellar structure, typical for thermally sprayed coatings, can be encountered in this coating, indicating an incomplete melting of the feed powder during the spraying process. This results in a rather high amount of porosity in the coating A as compared to the other studied coating. This porosity incorporated in coating A, in turn, results in thicker coatings. No marks of intense oxide layer formation on the surface of the powder particles during the spraying process utilising the lower operation temperature can be observed. As the spraying temperature rises, the lamellarity of coating structure increases, as can be assessed from Fig. 2(c). This is due to more efficient melting of the feed powder during the spraying event and it brings about a reduced amount of porosity in coating. The oriented lamellar structure is, thus, more pronounced in Al–Co–Fe–Cr coating B than in the coating A. Besides the tendency towards the build-up of a layered structure, the oxidation of powder particles is enhanced with an increasing spraying temperature, introducing oxide particles or even films into the HVOF sprayed coating B. The oxide particles are mostly located between the lamellas, as can be seen in Fig. 2(c). It is worth noting that there is no difference in the coating structure near the substrate and near the coating surface, thus, the coating structures were horizontally quite homogeneous.

The observations concerning the porosity as well as the presence of oxide particles and films in the Al–Co–Fe–Cr coatings were further confirmed with the elemental X-ray mapping. The elemental X-ray maps are collected for Al, Co, Fe, Cr and O for the studied coatings. The results of the elemental X-ray mapping for the coating A are shown in Fig. 3, while those for coating B are illustrated in Fig. 4. The X-ray maps indicate oxide particles to be composed of all the elements present in the powder (not only aluminium), since at least low elemental intensities are gained for all of them at the areas of great oxygen intensity. Moreover, in addition to this oxide formation, both the studied coatings comprise one phase only. This can be noticed from the even distribution of the mapped elements in the oxygen-free areas of the studied Al–Co–Fe–Cr coatings.

The composition of the phases present in Al–Co–Fe–Cr coatings was determined by the EDS analysis. As already

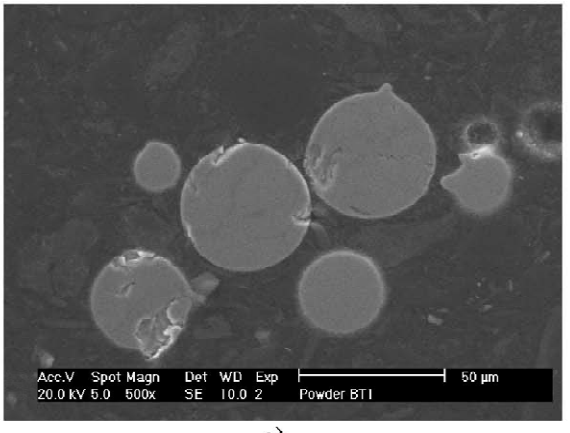

a)

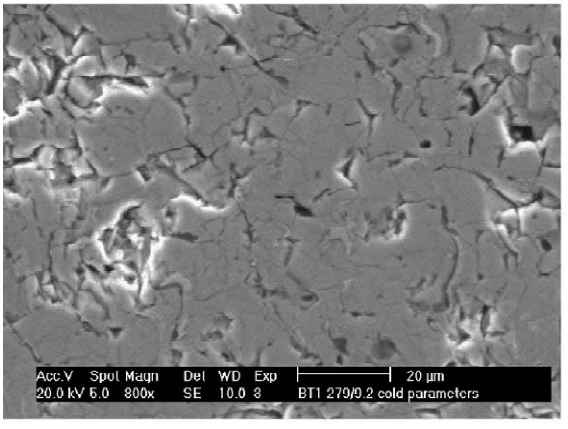

b)

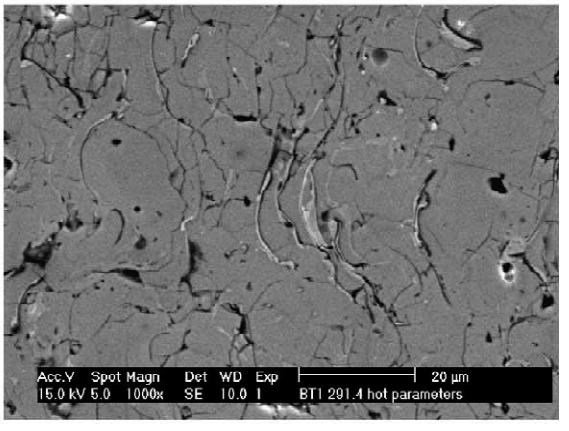

c)

Fig. 2. SEM photographs showing the microstructural details of Al–Co–Fe–Cr feed powder and HVOF sprayed coatings. (a) The morphology and microstructure of Al–Co–Fe–Cr feed powder BT1. (b) The microstructure of Al–Co–Fe–Cr coating A deposited with the lower spraying temperature. (c) The microstructure of Al–Co–Fe–Cr coating B deposited with the higher spraying temperature.

shown, coating A is mainly composed of one phase. The composition of this phase was determined to be 70.5 at.% Al, 12.5 at.% Co, 9.6 at.% Fe and 7.4 at.% Cr. The composition of this phase, accordingly, approximately corresponds to the composition of the feed powder. In the coating B, two main phases were identified. The composition of the major phase was 70.4 at.% Al, 12.5 at.% Co, 9.6 at.% Fe and 7.5 at.% Cr. The coating lamellas were built up of this phase. The other phase was principally located between the lamellas and contained a lot of oxygen. The oxide particle formation discussed above refers to the formation of this phase. The composition of this oxide phase was 41.4 at.% O, 47.8 at.% Al, 4.5 at.% Co, 3.2 at.% Fe and 3.1 at.% Cr. The oxide phase, thus, is somewhat enriched with aluminium as compared to the original composition of the feed powder. The oxide phase can still be considered as an oxidised form of the major phase, since not only aluminium but also the other elements oxidise during the spraying process. However, some oxide particles contained somewhat lower aluminium and higher alloying element concentrations. Cobalt concentrations as high as 23.5 at.% were measured. For iron and chromium, even 16.6 at.% and 11.6 at.% concentrations were determined, respectively. The rest of the phase was covered by aluminium and oxygen, the lowest aluminium content being 46.1 at.%. These oxide particles with lower aluminium content are suggested to carry out the compensation of the aluminium enrichment and the successive deficiency of alloying elements in the majority of oxide particles.

The earlier studies discussing the microstructure of thermally sprayed quasicrystalline Al–Cu–Fe coatings report the deficiency of Al during the spraying operation. This is due to the higher vapour pressure of Al as compared to the other two elements in Al–Cu–Fe feed powders [20,26,27]. Similarly in Al–Co–Fe–Cr feed pow-

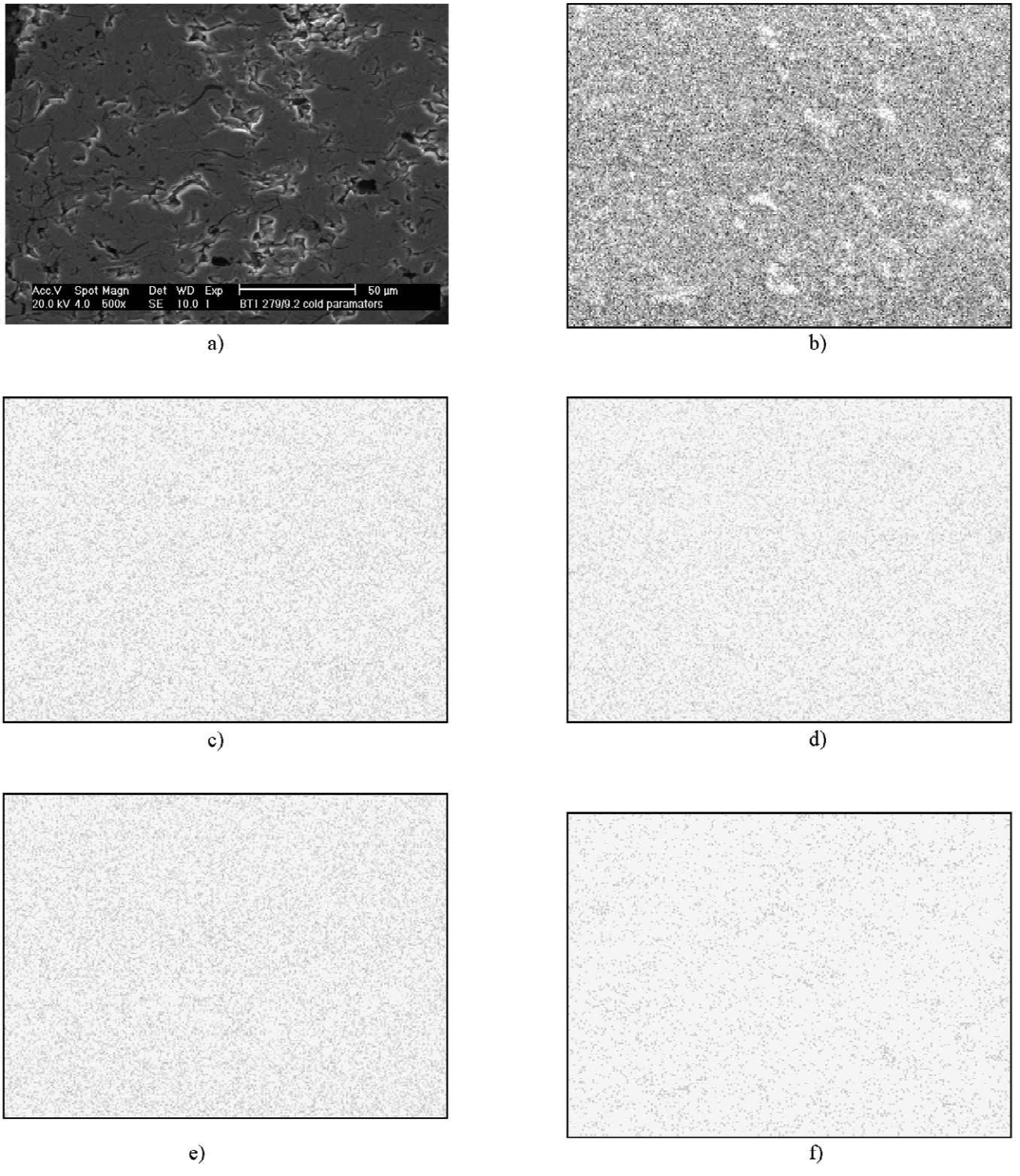

Fig. 3. The polished cross-section of the Al–Co–Fe–Cr coating A studied with the elemental X-ray mapping, (a) SEM micrograph showing the lamellar microstructure of the coating and the region for elemental mapping. (b) The aluminium map for the area. (c) The cobalt map for the area. (d) The iron map for the area. (e) The chromium map for the area. (f) The oxygen map for the area.

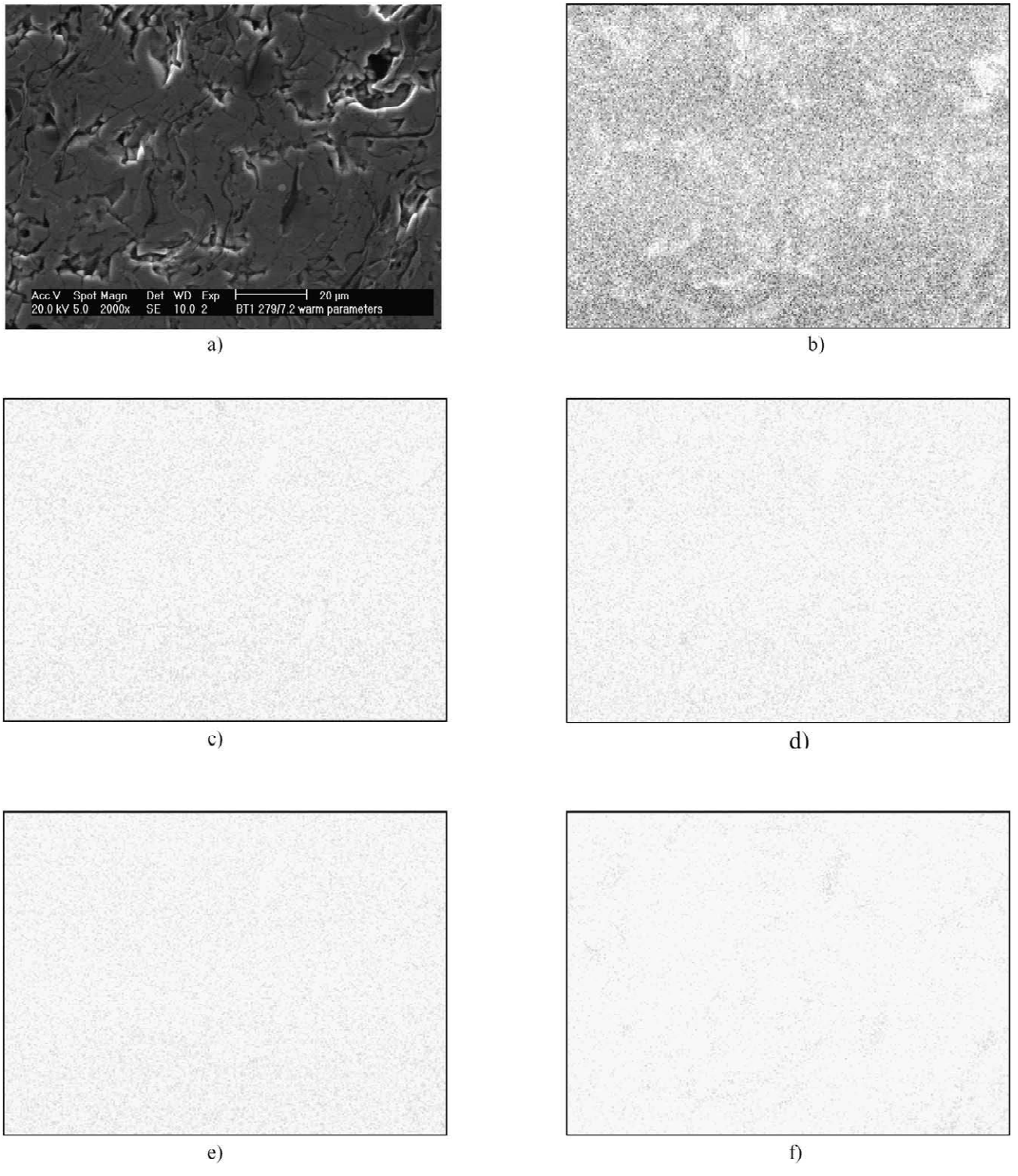

Fig. 4. The polished cross-section of the Al–Co–Fe–Cr coating B studied with the elemental X-ray mapping. (a) SEM micrograph showing the lamellar microstructure of the coating and the region for elemental mapping. (b) The aluminium map for the area. (c) The cobalt map for the area. (d) The iron map for the area. (e) The chromium map for the area. (f) The oxygen map for the area.

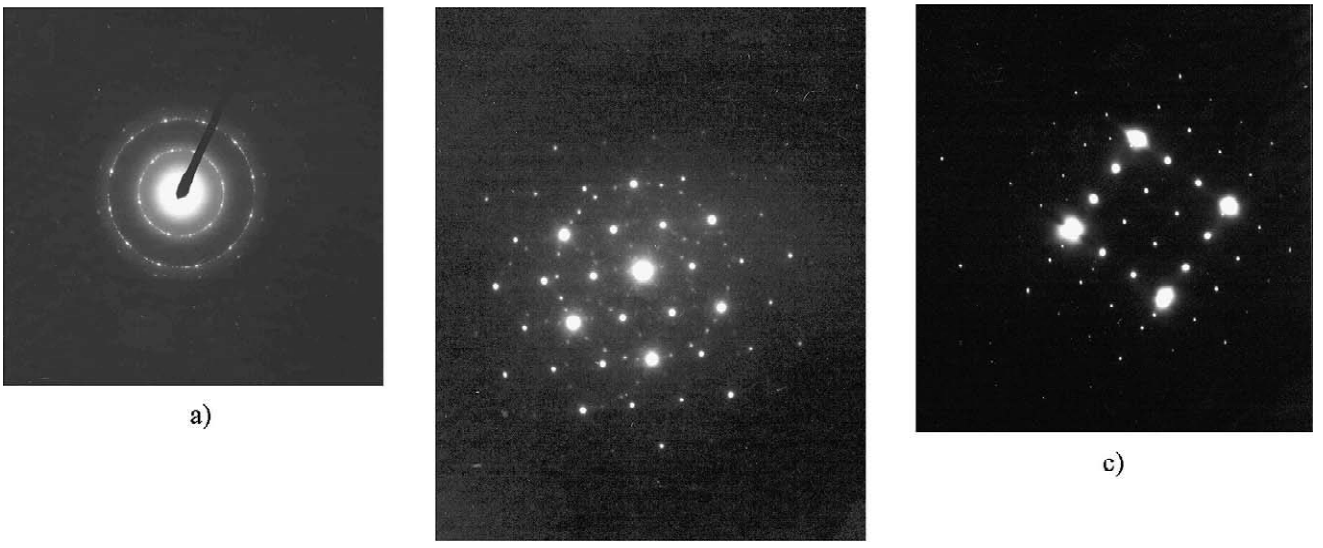

Fig. 5. Electron diffraction patterns of the dodecagonal quasicrystalline Al–Co–Fe–Cr phase taken along the (a) twelve-fold, (b) threefold and (c) twofold axes.

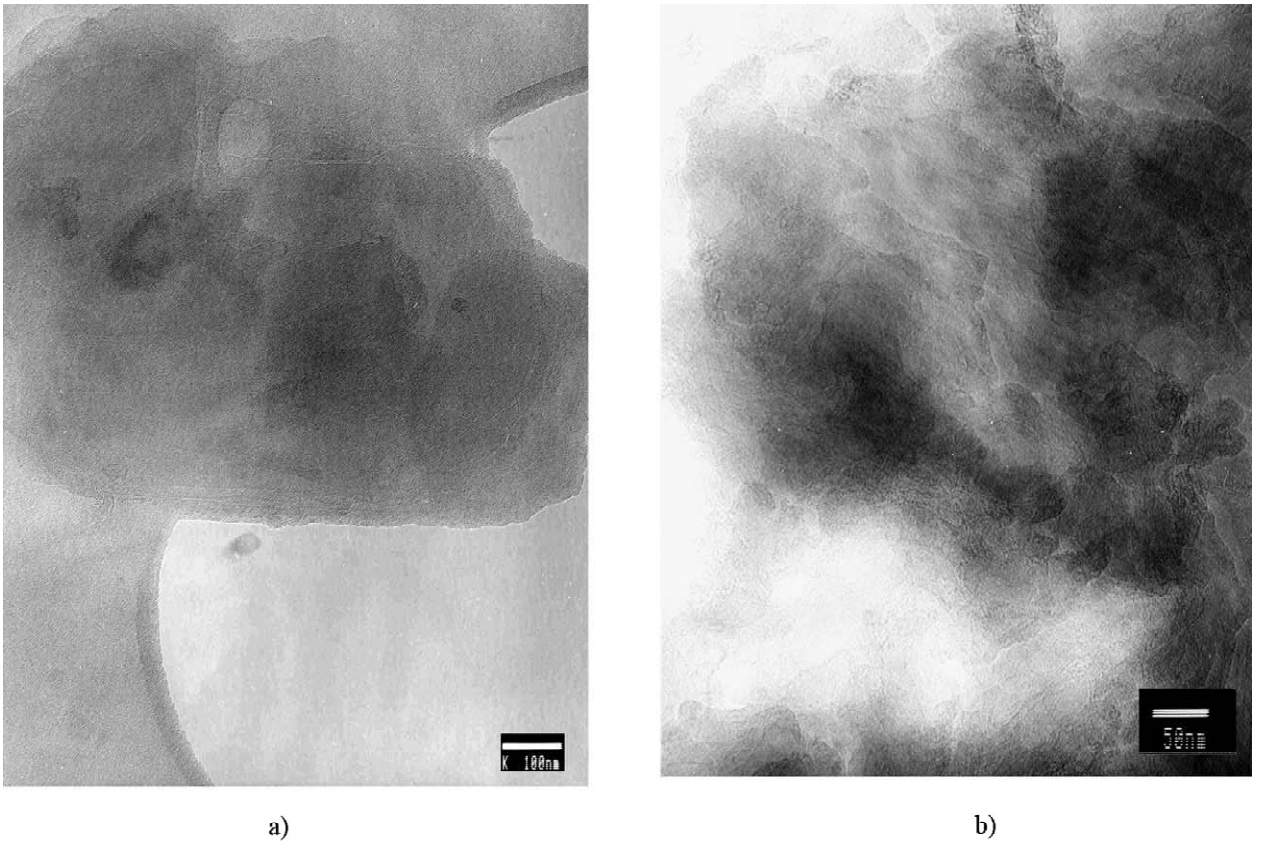

Fig. 6. (a) TEM bright field image of the feed powder particle showing the twelvefold symmetry. (b) TEM bright field image of the HVOF sprayed coating A showing the twelvefold symmetry. No defects or bend contours can be seen in the structure of this dodecagonal phase either in the feed powder or in the HVOF sprayed coatings. This is in agreement with the results of Sordelet et al. [27].

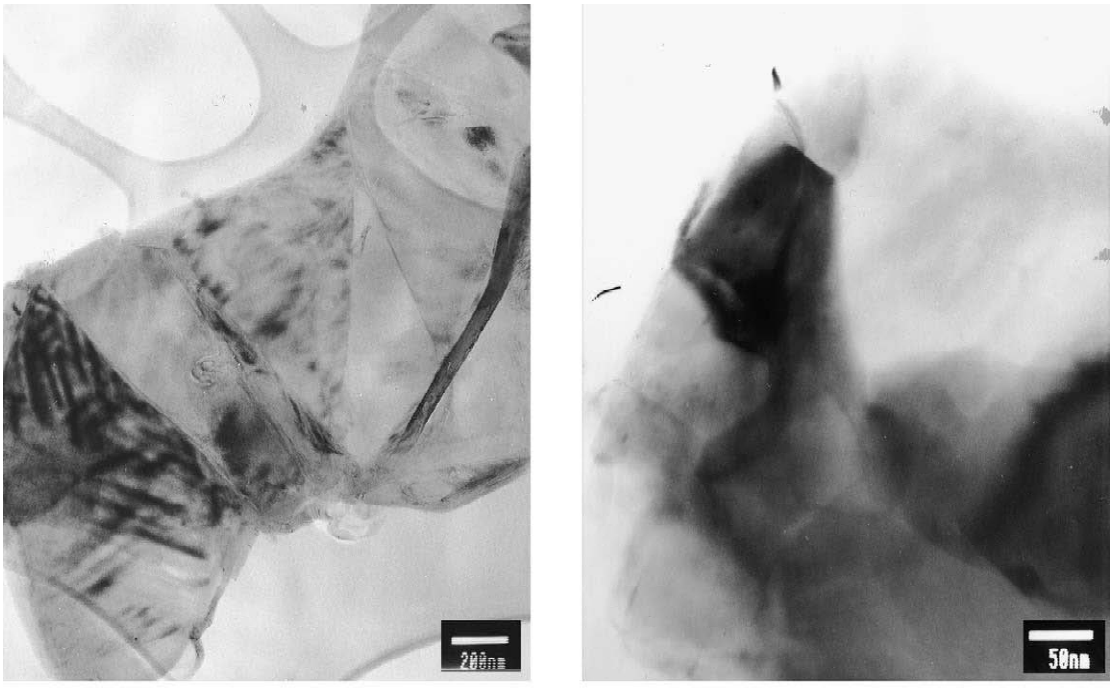

a) b)

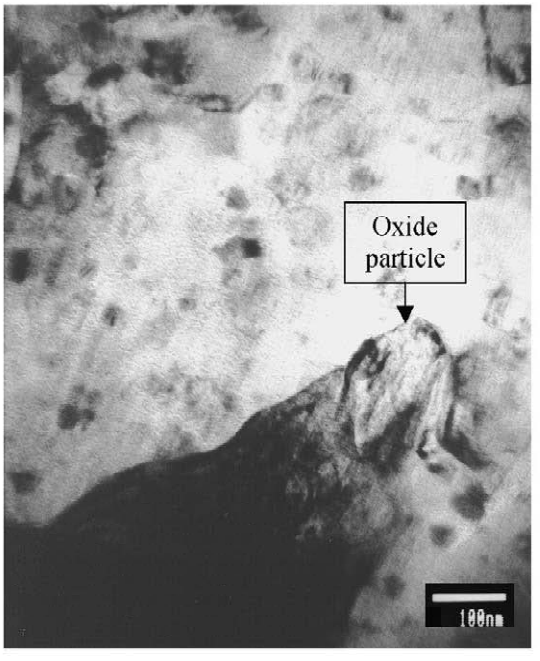

c)

Fig. 7. Microstructure of Al–Co–Fe–Cr coating B from different orientations. (a) TEM bright field image of the coating from the cross-sectional perspective. Micrograph taken with the electron beam parallel to the threefold axis. (b) TEM bright field image showing the coating structure from the top of the coating. Micrograph taken with the electron beam parallel to the twofold axis. (c) TEM bright field image showing the oxide particle in the coating structure. Micrograph taken with the electron beam parallel to the two-fold axis.

der of the present study, Al has a higher vapour pressure than the other elements. In this study, however, no such Al vaporisation was observed.

3.3. ATEM examination

The identification of the phases and their microstructure present in the feed powder and HVOF sprayed coatings was the main task of TEM studies. Also, the details of coating microstructure were of interest. TEM studies were carried out for the powdery samples; the feed powder was studied as such and the coating samples were crushed into a powdery form. The utilisation of the powdery samples instead of the cross-sections of coatings was due to the finding that the spraying process yields orientation into the coating structure [31], which may complicate the TEM studies.

TEM studies reveal the major phase in the feed powder and both of the HVOF sprayed coatings to be dodecagonal, since its diffraction pattern indicates a twelve-fold rotational symmetry. The indications of the presence of a quasicrystalline phase in studied structures due to XRD analysis were, thus, confirmed. Figs. 5(a)–(c) shows the twelve-fold, threefold and twofold zone axes patterns, respectively. The earlier studies of coating formation from the Al–Co–Fe–Cr powder have reported the formation of a decagonal quasicrystalline phase [28,29]. Instead, no observations of a dodecagonal phase have been announced. This finding of a new dodecagonal Al–Co–Fe–Cr phase greatly widens the family of dodecagonal quasicrystals, which has only embraced dodecagonal Co–Cu [32], Ta–Te [33], Ni–Cr [34], Ni–V and Ni–V–Si [35] alloys so far.

The microstructure of the feed powder particle with a twelvefold symmetry is shown in Fig. 6(a). A similar microstructure is retained in both of the coatings, too. Fig. 6(b) presents the section of the powder particle of coating A, exhibiting the twelvefold symmetry. It is worth noting that no defects can be seen in the structure of this dodecagonal phase either in the feed powder or in the HVOF sprayed coatings. This is in agreement with the results of Sordelet et al. [27]. Furthermore, the absence of phason strains, i.e. the sharpness of the diffraction spots, supports this finding.

Fig. 7 shows the microstructure of HVOF sprayed coating B from the cross-sectional perspective and from the top of the coating. As can be seen in Fig. 7(a), the coating lamellas consist of columnar grains extending through the lamella thickness. The columnar grains are approximately equiaxed on the plane parallel to the lamellas. In turn, the size of the grains somewhat varies throughout the coating structure; the diameter of the grains was generally 150–500 nm. This is also shown in Fig. 7(b).

Similarly to SEM studies, EDS analysis in TEM characterisation revealed no significant differences in the composition of the dodecagonal phase between the feed powder or the HVOF sprayed coatings. In the feed powder, the dodecagonal phase consisted of 64.5 at.% Al, 12.0 at.% Co, 8.9 at.% Fe, 7.5 at.% Cr and 7.1 at.% O. In the coating A, the dodecagonal phase contained 72.4 at.% Al, 10.2 at.% Co, 8.0 at.% Fe, 6.5 at.% Cr and 2.8 at.% O. The corresponding phase composition in the coating B was 72.2 at.% Al, 10.2 at.% Co, 8.0 at.% Fe, 5.8 at.% Cr and 4.4 at.% O. Accordingly, somewhat higher Al contents were received in TEM characterisation than in the SEM analyses. The main feature, however, to be taken into account is the involvement of oxygen in the EDS analysis of the dodecagonal phase. The presence of oxygen in the EDS analysis and in TEM analysis but not in SEM exploration indicates that the small and powdery TEM samples have oxidised due to their high surface area. Thus, oxygen can not be registered as a component element of the dodecagonal quasicrystalline phase, although it has earlier been described as a part of quasicrystalline Al–Cu–Fe–Cr–O structure [28,29].

In the feed powder and the HVOF sprayed coating A, no phases other than the dodecagonal one were encountered in the TEM studies. On the contrary, coating B, sprayed with higher operation temperature, contained an oxygen-containing minor phase together with the dodecagonal major phase. Particles of this oxygen-containing phase were predominantly located between the coating lamellas, as shown in Fig. 2(c), or even between the individual grains, as depicted in Fig. 7(c). The EDS analysis suggests the oxygen-containing phase to be composed of 48.0 at.% Al, 11.0 at.% Co, 8.2 at.% Fe, 6.2 at.% Cr and 26.7 at.% O. Similarly as in the SEM studies, also the Al-poor and alloying-element-rich version of the oxygen-containing phase was noticed in the TEM exploration of coating B. A concentration as low as 41.0 at.% was measured for aluminium in this Al-poor oxide, while cobalt concentrations as high as 21.0 at.%, iron contents as high as 15.1 at.% and chromium amounts as high as 12.7 at.% were measured. It is, still, worth noting that the amount of this Al-poor oxide is not high.

In the study of Sordelet et al. [26], the composition of the oxygen-containing phase was evaluated to be Al_2O_3. The results of the present study do not support this conclusion. Already the elemental X-ray maps recorded by SEM suggest the oxide-containing phase to be composed of all the elements present in the Al–Co–Fe–Cr alloy. Yet, no pure Al_2O_3 could be identified in XRD, SEM or TEM characterisation of the Al–Co–Fe–Cr coatings of the study. The results of TEM exploration also indicate the presence of all the alloy elements in the oxygen-containing phase. Besides, at the areas of high oxygen content, the dodecagonal quasicrystalline structure can still be resolved in the EDP. This promotes another theory of Sordelet et al. [27], where the oxygen is

presented to be present as a metallic oxide surface film on prior splat boundaries rather than as an interstitial solution or a precipitated oxide phase. However, more detailed studies are needed to characterise the structure of the oxygen-containing phase.

4. Conclusions

The microstructural characterisation was carried out for the Al–Co–Fe–Cr feed powder and the coatings sprayed with a HVOF method in order to explore the structural development of thick Al–Co–Fe–Cr coatings and the influence of the spraying parameters on the microstructure of produced Al–Co–Fe–Cr coatings. The results show that Al–Co–Fe–Cr feed powder and the coatings sprayed with lower and higher operation temperatures are all composed of a dodecagonal quasicrystalline phase. The composition of this new dodecagonal phase approximately corresponds to that of a feed powder, being $Al_{70.6}Co_{12.5}Fe_{9.4}Cr_{7.5}$. This finding of a new dodecagonal Al–Co–Fe–Cr phase greatly widens the family of existing dodecagonal quasicrystals, which, so far, has only embraced alloys Co–Cu, Ta–Te, Ni–Cr, Ni–V and Ni–V–Si.

The dodecagonal phase orientates during the spraying process. As a result, a lamellar coating structure forms with both used spraying temperatures. These lamellas are made up of columnar dodecagonal grains, which extend through the lamella thickness. However, the melting of powder particles and the subsequent build-up of an oriented lamellar structure is not complete when a lower spraying temperature is used, yielding porosity into the coating. Higher spraying temperature, in contrast, promotes oxidation, leading to the incorporation of an oxygen-containing film on splat boundaries. Thus, while feed powder and the coating deposited with a lower spraying temperature are one-phase structures, the coating sprayed with a higher operation temperature is comprised of a dodecagonal phase and an oxygen-containing phase. The oxygen-containing phase is not pure aluminium oxide but contains all the elements present in the alloy.

It should be noticed that among quasicrystalline powders the studied dodecagonal Al–Co–Fe–Cr powder was exceptionally easy to spray with a HVOF method due to its structural stability. No phase transformations typical for metastable quasicrystals were associated with the HVOF spraying of Al–Co–Fe–Cr powder at the studied temperatures. Similarly, no vaporisation of Al, typical for some less stable quasicrystalline powders, was observed for the Al–Co–Fe–Cr alloy. The spraying parameters were mainly observed to regulate the porosity and, thus, thickness as well as the amount of the oxidised splat boundaries of Al–Co–Fe–Cr coatings.

Acknowledgements

E. H.-S. expresses her sincere thanks to the Academy of Finland and Walter Ahlström Foundation for financing her research.

References

[1] D.J. Sordelet, J.M. Dubois, Mater. Res. Soc. Bull. 11 (1997) 34–37.
[2] D. Shechtman, I. Blech, D. Gratias, J.W. Cahn, Phys. Rev. Lett. 53 (1984) 1951–1953.
[3] A.P. Tsai, Mater. Res. Soc. Bull. 11 (1997) 43–47.
[4] K. Kimura, H. Yamane, T. Hashimoto, S. Takeuchi, Mat. Sci. Eng. A 99 (1988) 435–438.
[5] C. Suiyanarayana, Prog. Mater. Sci. 46 (2001) 1–184.
[6] F. Schurack, J. Eckert, L. Schultz, Mater. Sci. Eng. A 294–296 (2000) 164–167.
[7] J. Eckert, L. Schultz, K. Urban, Mater. Sci. Eng. A 133 (1991) 393–397.
[8] M. Takeda, S. Sakai, A. Kawasaki, Y. Hattori, M. Katoh, Mater. Sci. Eng. A 294–296 (2000) 842–845.
[9] R. Teghil, L. D'Alessio, M.A. Simone, M. Zaccagnino, D. Ferro, D.J. Sordelet, Appl. Surf. Sci. 168 (2000) 267–269.
[10] Y. Ding, D.O. Northwood, A.T. Alpas, Surf. Coatings Tech. 96 (1997) 140–147.
[11] A. Kanjilal, U. Tiwari, R. Chatterjee, Mater. Res. Bull. 37 (2002) 343–351.
[12] T. Grenet, F. Giroud, K. Loubet, A. Bergman, G. Safran, J. Labar, P. Barna, J.L. Joulaud, M. Capitan, J. Alloys Comp. 342 (2002) 2–6.
[13] C.J. Jenks, P.A. Thiel, Mater. Res. Soc. Bull. 11 (1997) 55–58.
[14] J.M. Dubois, Mater. Sci. Eng. A 294–296 (2000) 4–9.
[15] E. Belin-Ferré, J.M. Dubois, V. Fournée, P. Brunet, D.J. Sordelet, L.M. Zhang, Mater. Sci. Eng. A 294–296 (2000) 818–821.
[16] P. Brunet, L.M. Zhang, D.J. Sordelet, M. Besser, J.M. Dubois, Mater. Sci. Eng. A 294–296 (2000) 74–78.
[17] F. Audebert, R. Colaco, R. Vilar, H. Sirkin, Scr. Materialia 40 (1999) 551–557.
[18] B. Wolf, K.O. Bambauer, P. Paufler, Mater. Sci. Eng. A 298 (2001) 284–295.
[19] D.J. Sordelet, M.F. Besser, J.L. Logsdon, Mater. Sci. Eng. A 255 (1998) 54–65.
[20] M.F. Besser, T. Eisenhammer, Mater. Res. Soc. Bull. 11 (1997) 59–63.
[21] E. Fleury, Y.-C. Kim, J.-S. Kim, H.-S. Aim, S.-M. Lee, W.-T. Kim, D.-H. Kim, J. Mater. Res. Soc. 17 (2002) 492–501.
[22] D.J. Sordelet, M.F. Besser, J.L. Logsdon, Mater. Sci. Eng. A 255 (1998) 54–65.
[23] E. Fleury, Y.-C. Kim, J.-S. Kim, D.-H. Kim, W.-T. Kim, H.-S. Ahn, S.-M. Lee, J. Alloys Comp. 342 (2002) 321–325.
[24] D.J. Sordelet, S.D. Widener, Y. Tang, M.F. Besser, Mater. Sci. Eng. A 294–296 (2000) 834–837.
[25] S. De Palo, S. Usmani, S. Sampath, D.J. Sordelet, M. Besser, in: C.C. Berndt (Ed.), Thermal Spray: A United Forum for Scientific and Technological Advances, ASM International, Ohio, USA, 1997, pp. 135–139.
[26] D.J. Sordelet, M.F. Besser, I.E. Anderson, J. Thermal Spray Tech. 5 (1996) 161–174.
[27] D.J. Sordelet, M.J. Kramer, O. Unal, J. Thermal Spray Tech. 4 (1995) 235–244.
[28] J. Reyes-Gasga, A. Pita-Larranaga, M.P. Valles-Gonzalez, A. Sanchez-Pascual, Thin Solid Films 355–356 (1999) 506–512.
[29] J. Reyes-Gasga, A. Pita-Larranaga, G. Mondragon-Galicia, M.P. Valles-Gonzalez, A. Sanchez Pascual, Mater. Sci. Eng. A 294–296 (2000) 850–853.

[30] L. Pawlowski, The Science and Engineering of Thermal Spray Coatings, John Wiley & Sons, Chichester, England, 1995.
[31] X.Z. Li, L.D. Marks, J. Maciejewski, L. Fehrenbacher, J. Zabinski, J. O'Neill, Metall. Mater. Trans. A 33 (2002) 675–679.
[32] Z.F. Li, B.X. Liu, Nucl. Instr. Methods Phys. Res., B 178 (2001) 224–228.
[33] M. Uchida, S. Horiuchi, Micron 31 (2002) 493–497.
[34] T. Ishimasa, H.-U. Nissen, Y. Fukano, Phys. Rev. Lett. 55 (1985) 511–513.
[35] H. Chen, D.X. Li, K.H. Kuo, Phys. Rev. Lett. 60 (1988) 1645–1648.